We are IntechOpen, the world's leading publisher of Open Access books Built by scientists, for scientists

6,900
Open access books available

186,000
International authors and editors

200M
Downloads

Our authors are among the

154
Countries delivered to

TOP 1%
most cited scientists

12.2%
Contributors from top 500 universities

WEB OF SCIENCE™

Selection of our books indexed in the Book Citation Index in Web of Science™ Core Collection (BKCI)

Interested in publishing with us?
Contact book.department@intechopen.com

Numbers displayed above are based on latest data collected.
For more information visit www.intechopen.com

5

Comparative Study of Membranes Obtained from PA6 and PA66/National Clay Nanocomposites

Amanda M. D. Leite, Edcleide M. Araújo, Vanessa da N. Medeiros, Rene A. da Paz and Hélio de L. Lira
Federal University of Campina Grande (CCT/UAEMa/Bloco CL)
Brazil

1. Introduction

Polyamide is an important group of the thermoplastic excellent solvent resistance and good processability. However, polyamide exhibits a relatively rapid crystallization rate, which makes it to have some drawbacks such as high mold shrinkage and dimensional instability. In order to control the crystallization rate and the crystallinity, then achieve the desired morphology and properties, a great deal of efforts has been made on studying the crystallization kinetics corresponding to the change of the performed properties (Liu & Yang, 2009; Lu et al.,,2001; Run et al., 2005).

Composite materials are widely used in various fields, such as the automotive industry, aeronautics, and communications. Depending on the composite nature and structure, many properties can be improved: hardness, tenacity, deformation temperature, price, and so forth. Nanocomposites refer to composites in which one of the components has at least one dimension of about a few nanometers. They are a relatively new class of material. The nanoscale dispersion gives better mechanical properties. A few articles focus on the advantages of using nanocomposites (Varlot et al., 2001).

Polymer nanocomposites are an area of substancial scientific interest and of emerging industrial practice. Hybrid combinations of natural fillers and polymers were presented to the public for the first time in 90s (Pfaendner, 2010). In recent years, the dispersion of low loadings (ca. 5%) of inorganic particles in the nanosize scale in organic polymers is a challenge for the preparation of new composite materials with enhanced mechanical, gas barrier and flame retardant properties, when compared to those of composites prepared with micron size particles. A homogenous dispersion of nanoparticles is believed to contribute better to the property improvement (Herrero et al., 2010; Dubois, 2000).

Although fillers like alumina, silica, etc., can be added, layered inorganic compounds possess unique properties to be active as fillers in polymeric nanocomposites. They can be, in fact, exfoliated into single layers, each of them having a thickness of the order of nanometers (from ca. 0.7 to 2.5 nm) and by ion exchange or grafting reactions the surface of the layers may be functionalized with organic groups that increase the compatibility with the polymers (Herrero et al., 2010). In addition, layered solids may intercalate polymeric chains in their interlayer regions. Until now, however, the clay materials involved in this

field have been mostly focused on montmorillonite-type layered silicates whose layers have a relatively low charge density and from which exfoliated montmorillonite-type layered silicate/polymer nanocomposites can be easily obtained (LeBaron et al., 1999; Lagaly, 1999).
Montmorillonite is one of the most commonly used clay minerals in polymer nanocomposites, due to its high cation exchange capacity, excellent swelling ability, high aspect ratio and ease for modification (Xi et al., 2005). However, it is very difficult for the hydrophilic montmorillonite to be exfoliated and well-dispersed in a hydrophobic polymer matrix. Therefore, two main objectives for modification are: to expand the interlayer space of the clay, allowing large polymer molecules to enter into the interlayer space, and to improve the miscibility of clay with the polymer, thereby achieving a good dispersion of clays in the polymer matrix (Zhao et al., 2010).
Several methods have been developed to produce clay/ polymer nanocompósitos (Dubois,2000). Three methods were developed in the early stages of this field and have been applied widely. These are: in situ polymerization (Wang et al., 2005), solution induced intercalation (Qiu et al., 2006), and melt processing (Lee et al., 2006).
A membrane is an interphase between two adjacent phases acting as a selective barrier, regulating the transport of substances between the two compartments. The main advantages of membrane technology as compared with other unit operations in (bio)chemical engineering are related to this unique separation principle, i.e. the transport selectivity of the membrane. Separations with membranes do not require additives, and they can be performed isothermally at low temperatures and—compared to other thermal separation processes—at low energy consumption (Ulbricht, 2006). The primordial function of a membrane is to act as a selective barrier, allowing the passage of certain components and the retention of others from a determined mixture, implying the concentration of one or more components both in the permeate and in the retentate. Its selectivity is related to the dimensions of the molecule or particle of interest for separation and the pore size, as also the solute diffusivity in the matrix and the associated electric charges (Coutinho et al., 2009).
The separation performance of a membrane is influenced by its chemical composition, temperature, pressure, feed flow and interactions between components in the feed flow and the membrane surface (Lin, et al., 1997).
The membranes can be classified as symmetrical or asymmetrical. This asymmetry is considered with respect to the internal structure of the membranes. Symmetrical membranes show uniform pore sizes in their cross-section whereas the pores of asymmetric membranes are usually larger the further they are from the filter surface. In general the most important characteristics of membranes are: thickness, pore diameter, solvent permeability and porosity. Other important parameters are: permeate flow rate, heat, chemical and mechanical resistance (Coutinho et al., 2009). From the morphological point of view, membranes can be divided into two large categories: dense and porous. Membranes are considered to be dense when transport of the components involves a stage of dissolution and diffusion across the material constituting the membrane. On the other hand a membrane is denominated as porous when permeate transport occurs preferentially in the continuous fluid phase which fills the membrane pores (Habert, Borges, & Nobrega, 2006).
Several industrial separation processes make use of polymeric membranes. When porous polymeric membranes are needed, phase separation of polymer solutions is the fabrication method of choice. First, a polymer solution is cast on a support. Then, the phase separation can be induced by means of contacting the polymer solution with a suitable non-solvent in

the liquid or vapor phase (liquid induced phase separation or vapor induced phase separation). Diffusional exchange of solvent and non-solvent induces a thermodynamic instability in the polymer solution causing phase separation to occur into a polymer-rich phase and a polymer-lean phase. The polymer-rich phase forms the body of the membrane, whereas the polymer-lean phase will form the porosity inside the membrane. The morphology of the membrane depends strongly on the conditions under which the phase separation is carried out (Boom et al., 1992; Witte et al., 1996; Bulte et al., 1996).

Adding the inorganic nanoparticles into polymeric materials to improve the filtration membrane properties has attracted broad attentions in the development of membrane science and technique. Many literatures (Yang et al., 2007; Uragami et al., 2005; Nagarale et al., 2005) indicated that adding proper inorganic nanoparticles in polymeric casting solution could suppress the formation and growth of macrovoids, to increase the number of small pores and run-through pores, to improve the porosity, hydrophilicity and permeability with almost unchanged retention, and to enhance the mechanical and thermal stabilities and the anti-fouling performance.

Therefore, the aim of this work was to evaluate the thermal behavior of microporous membranes obtained from nanocomposites of PA6 and PA66/national clay.

2. Experiment

2.1 Materials

Bentonite clay Brasgel PA (sodium), with CEC (cation exchange capacity) = 90 meq/100 (method of adsorption of methylene blue) passed through ABNT sieve no. 200 (D = 74μm), cream colored, supplied by Bentonit União Nordeste (BUN) located in Campina Grande-PB. The polymer matrix used was a polyamide 6 (Technyl C216) and polyamide 66 (Technyl A216) provided by Rhodia/ SP, in the form of white pelets. It was used the Genamin (hexadecyltrimethylammonium chloride) quaternary ammonium salt, produced by Clariant/PE. For the preparation of membranes, it was used the formic acid solvent at 99% by Vetec/SP.

2.2 Methodology

To make the clay compatible with the polymer matrix, the sodium ions present between the layers of clay were exchanged for ions of the quaternary ammonium salt (Genamin) to produce the organoclay, called OMMT. To obtain the organoclay (OMMT) a suitable treatment was suitable for the salt, based on the CEC of clay, according to procedure reported in previous studies (Leite et al., 2009; Araujo et al., 2007).

To obtain the nanocomposites of polyamide/clay there has been a preparation of concentrates (1:1) in an internal mixer coupled to a torque rheometer from Haake System 90-Büchler, operating at 240°C for polyamide 6 and 260ºC for polyamide 66, at 60 rpm for 10 minutes. The concentrates obtained were granulated and added to the polymer matrix in quantities necessary to obtain nominal concentrations of 3 wt% clay. The mixtures were processed in a counterrotating twin screw extruder coupled to a torque rheometer System 90 from Haake-Büchler at a temperature of 240°C for polyamide 6 and 260ºC for the polyamide 66 in all heating zones and speed of the screws at 60 rpm. Before any processing step, the polyamide materials were dried at 80 ± 5 º C for 24 hours in the vacuum oven before being processed for removal of moisture (Leite et al., 2009).

The method of phase inversion by immersion-precipitation technique was used in the preparation of membranes. Polyamide 6 and Polyamide 66 and the nanocomposites (dried

at 80°C under vacuum for a period of 24 hours) were dissolved in a quantity in weight of 20% polymer and 80% formic acid at a temperature of 40°C, until complete dissolution of the polymer. When dissolved in formic acid, polyamide forms a clear and homogeneous solution whereas nanocomposites form a turbid one. After being prepared, the solution was spread on a glass plate and then quickly immersed in a bath of distilled water, a non-solvent element. After completion of the precipitation, the membrane was removed and washed with distilled water then dried in an oven at 50°C for 2 hours.

2.3 Characterization

2.3.1 X-ray Diffraction (XRD)

The spacing basal of the samples was observed by X-ray diffraction (XRD) at room temperature by XRD-6000 Shimadzu diffractometer (40 kV, 30 mA) using CuKα radiation (λ = 0.154 nm) at the rate of 2° min-1 in the range of 2.0−30°.

2.3.2 Transmission Electron Microscope (TEM)

The phase morphologies of the nanocomposites were observed by transmission electron microscope (TEM), Philips CM 120, operating at an acceleration voltage of 120 kV. Samples were cryogenically microtomed (−80 °C) into ultrathin sections (~30 nm thick) from films with a diamond knife using a RMC MT-7000.

2.3.3 Scanning Electron Microscopy (SEM)

The structures of the membranes were characterized by SEM SSX 550 Superscan— Shimadzu, operating with 15 kV. All samples were gold sputtered.

2.3.4 Water flux

For the testing of water permeability, we used a perpendicular Amicon filtration cell (effective area = 28.7 cm^2), coupled to a filtration system (Figure 1). The membranes were tested for permeability at different pressures: 0.5 and 1.0 bar. The collections of permeated water was measured in an interval of 3 minutes, and each collection was made for a period of 1 minute

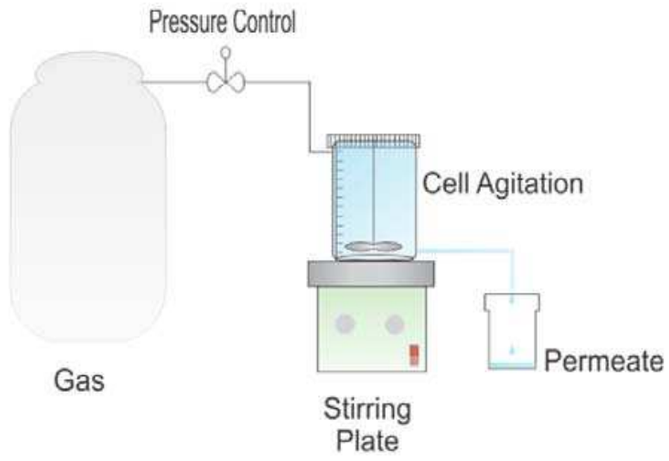

Fig. 1. Schematic representation of the used filtering system.

3. Results and discussion

3.1 X- Ray Diffraction of clay and nanocomposites (XRD)

The XRD patterns were made to the clay without treatment (MMT) and clay treated with Genamin. Figure 2 shows that there was a shift of the 2θ angle of 6.97° (MMT, d001 = 12.74 Å) to 4.01° (OMMT, d_{001} = 22.34 Å). The shift to smaller angles and, consequently, increasing the basal spacing, it indicates that the intercalation of molecules in the salt between the layers of clay. showing an expansion of the basal interplanar distance, indicating the intercalation of the salt in the clay. The interlayer distance is determined by the diffraction peak in the X-ray method, using the Bragg equation. The results indicated that the quaternary ammonium salt Genamin was intercalated between two basal planes of MMT, leading to an expansion of the interlayer spacing, conform reported too in others works (Fornes et al., 2001; Araujo et al., 2007) that used this quaternary ammonium salt in the organophilization of bentonite clays of same precedence.

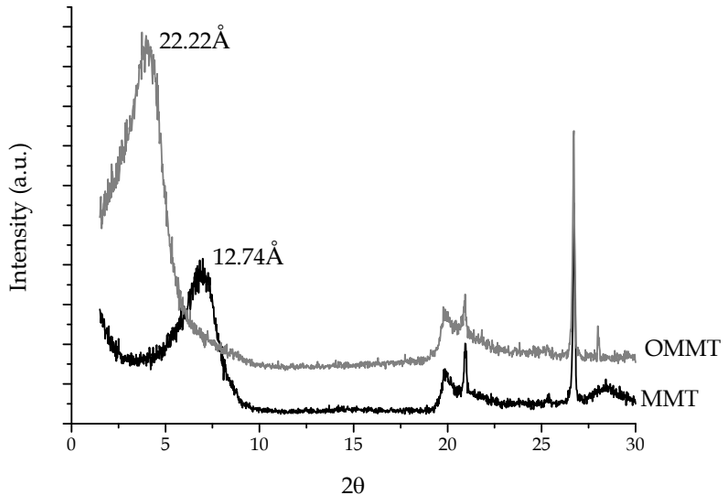

Fig. 2. XRD patterns of MMT and OMMT clays

Figure 3 (a and b) shows the X-ray diffraction patterns of clay without treatment (MMT), treated (OMMT), and the nanocomposites of polyamide 6 and 66. It is observed that the clay without treatment presents an interplanar basal distance of about 12.74 Å, a characteristic of the clay minerals in smectite group. Concerning treated clay there was a peak shift to lower angles in the order of 22.22 Å, showing an expansion of the basal interplanar distance, indicating the intercalation of the salt in the clay.

Regarding the nanocomposites of polyamide/clay that were analyzed through films, it can be observed that the characteristic peak of the treated clay no longer appears. This result shows that apparently the nanocomposites obtained present an exfoliated or partially exfoliated structure. This will then be confirmed by transmission electron microscopy.

3.2 Transmission Electron Microscopy (TEM)

The photomicrographs of Figure 4 (a and b) show the PA 6/MMT and PA 66/MMT systems. For the PA system 6/MMT presents a partially exfoliated morphology, composed of layers of clay and some clusters dispersed in the polymer matrix, since for

photomicrography 66/MMT PA system, there is a morphology composed predominantly of small and large clusters of lamellae of clay, ie a structure with partial intercalation, also called a microcomposite.

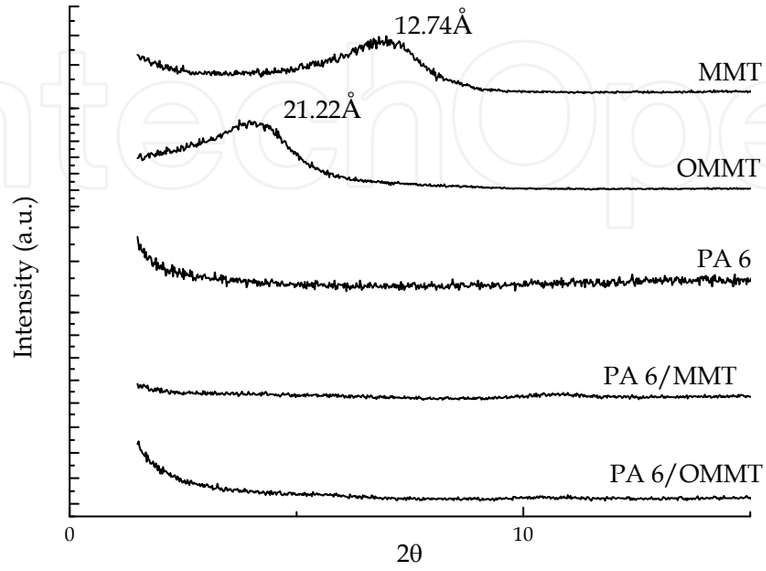

(a)

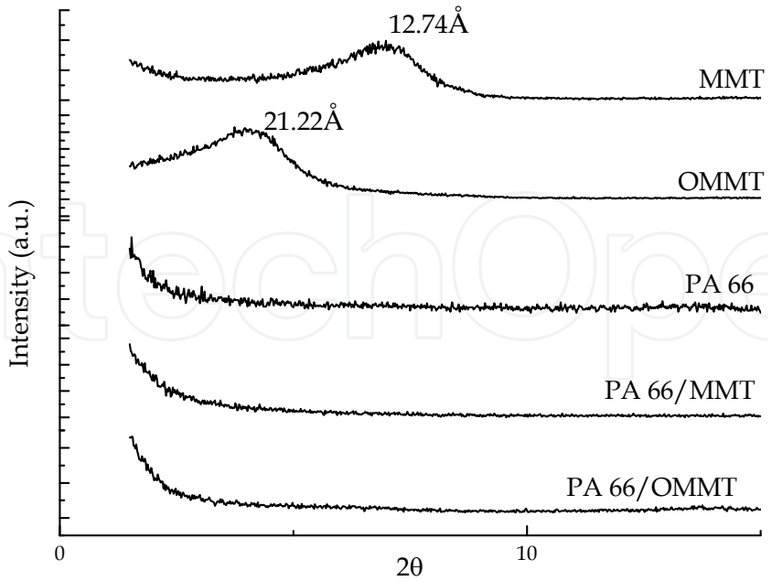

(b)

Fig. 3. XRD patterns of MMT and OMMT clays and nanocomposites of (a) PA 6 and (b) PA 66

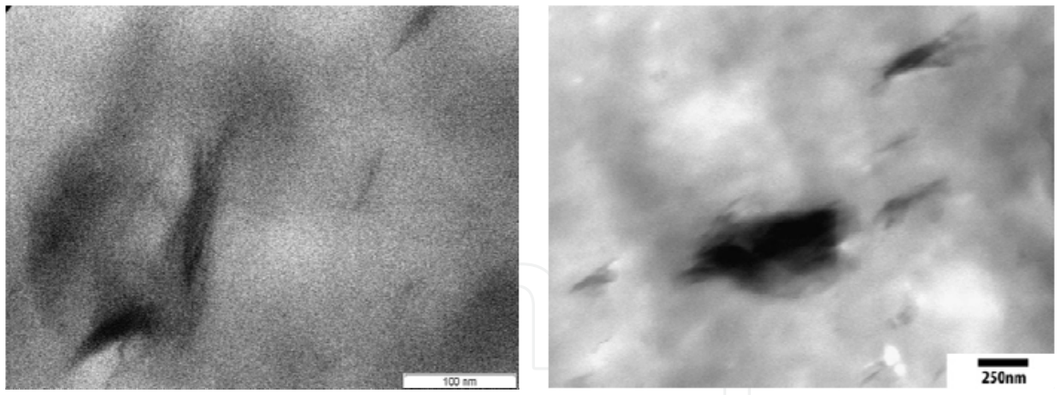

(a) (b)

Fig. 4. TEM photomicrographs of the nanocomposites films of (a) PA 6/MMT and (b) PA 66/MMT.

Figures 5a and b respectively show photomicrographs of nanocomposites of polyamide 6 and polyamide 66 with treated clay. Figure 5a makes it possible to observe a partially exfoliated morphology, composed of layers of clay and some clusters dispersed in the polymer matrix. Figure 5b presents a similar morphology however showing an absence of clusters. It apparently presents a more exfoliated morphology compared to nanocomposite polyamide 6/OMMT. In a general way, the quaternary ammonium salt studied favored the production of nanocomposites with a predominantly exfoliated structure, thus confirming the results of X-ray diffraction previously obtained and displayed.

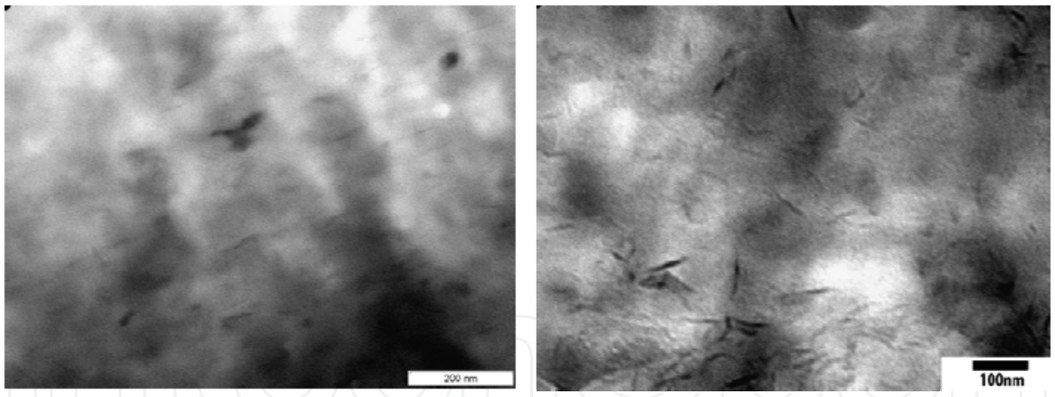

(a) (b)

Fig. 5. TEM photomicrographs of the nanocomposites films of (a) PA 6/OMMT and (b) PA 66/OMMT.

3.3 X- Ray Diffraction (XRD) of membranes

Figure 6 (b) shows the XRD diffractograms of the membranes prepared from polyamide 6 and 66 and its nanocomposites. According to what has been mentioned for the XRD diffractograms of the films obtained from the granules of nanocomposites, Figure 3, we can also emphasize here the disappearance of the characteristic peak of clay, confirming the exfoliation of the membranes produced from the nanocomposite , ie, behavior similar to that previously studied. Through these diffractograms, one can see the presence of two peaks at

2θ of about 20 ° and 24 ° for all compositions of the membranes. The appearance of both peaks may be related to the formation of a crystalline polyamide phase, called phase α (alpha) (Kohan, 1995).

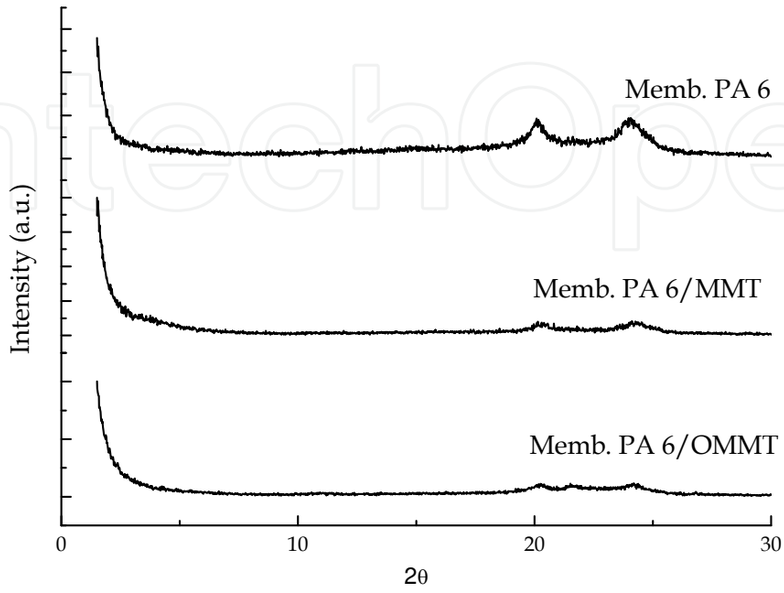

(a)

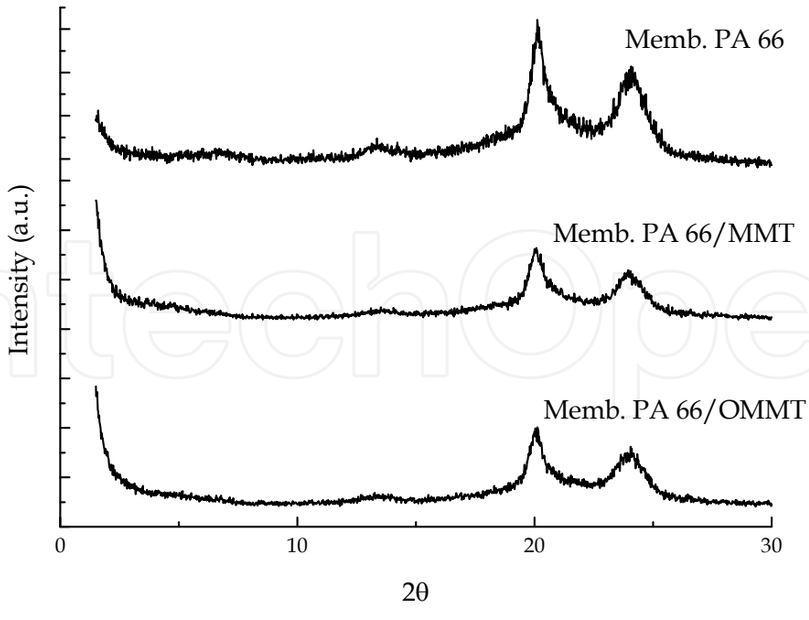

(b)

Fig. 6. XRD patterns of membranes obtained of (a) PA 6 and (b) PA 66

According to Khanna and Kuhn (1997), polyamide can take two crystallographic forms, α monoclinic and monoclinic or γ pseudo-hexagonal. In the α form, the hydrogen bonds are formed between antiparallel chains, and γ form between parallel chains by hydrogen bonds, causing the twist of the molecular chains in zig-zag planes. As a result of this phenomenon, the crystal density and heat of fusion of γ form, where interactions between the chains are weaker, are less than α form. The α way can be identified in XRD pattern of X-ray diffraction peak at 2 θ approximately 24°, the crystalline γ form is shown in diffractogram as a peak between 21 and 22. As seen, the introduction of clay and formic acid changes the shape of these peaks, probably by changing the crystallinity of PA.

3.4 Scanning Electron Microscopy (SEM)

3.4.1 Top surface

In Figure 7 (b) are shown photomicrographs of the top of the membranes of pure polyamide 6 and 66. For the membrane of polyamide 6, this surface is virtually skinless, composed of 'sheaf-like' crystallites, as in the membrane interior. The sizes of the crystallites are considerably smaller than those in Fig. 7(a), suggesting that there is a much higher nucleation density during precipitation in this top surface. Already the polyamide 66 membranes, presents a continuous skin composed of intersecting polygonal plates with approximately linearly boundaries. These crystalline plates resemble the two-dimensional spherulites commonly observed in melt-crystallized films.

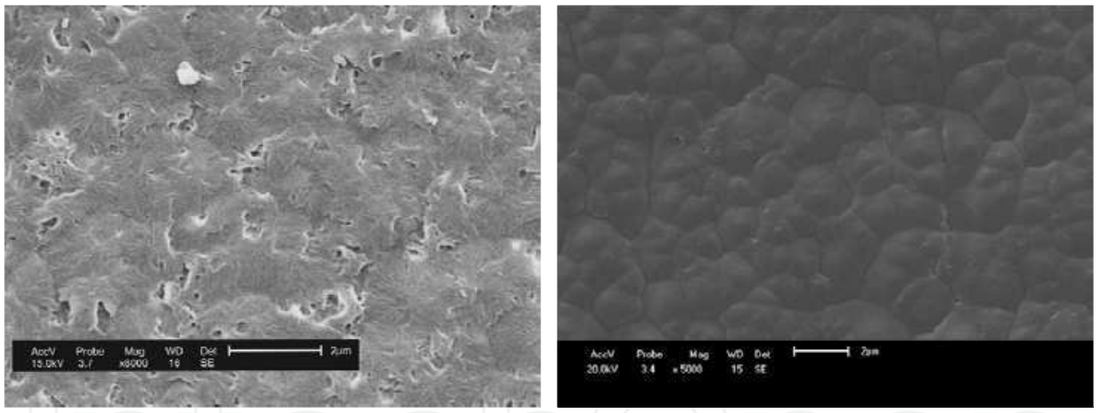

(a) (b)

Fig. 7. SEM images of the top surface of (a) PA 6 (b) PA 66

Figures 8 and 9 shows the photomicrographs of the top of the membranes obtained from nanocomposites of PA6 and PA66. Analyzing the images, it can be seen that the membranes obtained from the nanocomposites show a higher amount of pores and their distribution more uniformly compared to the membrane of PA 6. Moreover, it is observed that the presence of clay treated decreases pore size. As for the PA 66 membrane there is a behavior similar to the membrane of pure PA 66. It appears that for the membranes obtained from PA6 It shows the presence of particles to the membrane obtained from the pure polymer can be attributed to the presence of such a differential precipitation on the membrane surface or to an incomplete dissolution of the polymer during the preparation of the solution to obtain the membranes. The membranes with the presence of clay can be attributed to an incomplete homogenization of the clay with the polymer during preparation of the solution.

The agglomeration of the layers of clay, because of possible interactions of molecules present in the clay of the salt with formic acid. These clusters are seen macroscopically in the membrane where it was used nanocomposite with treated clay.

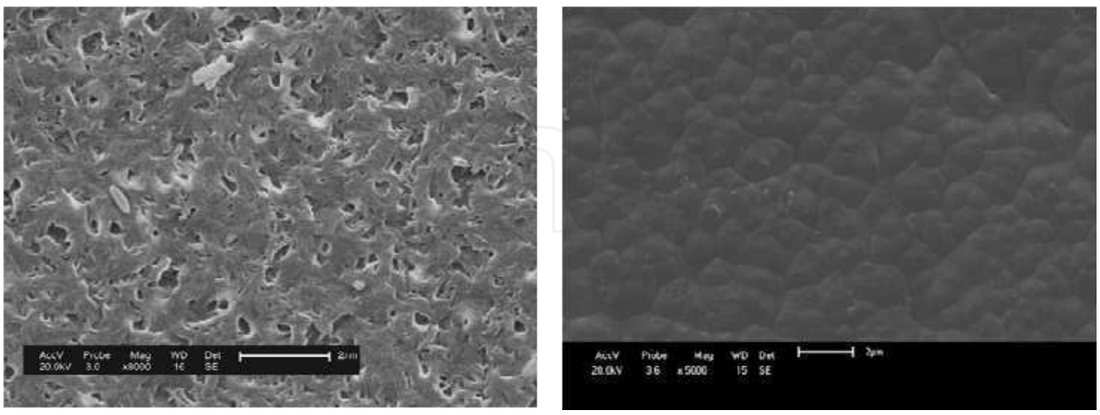

(a) (b)

Fig. 8. SEM images of the top surface of (a) PA 6/MMT (b) PA 66/MMT

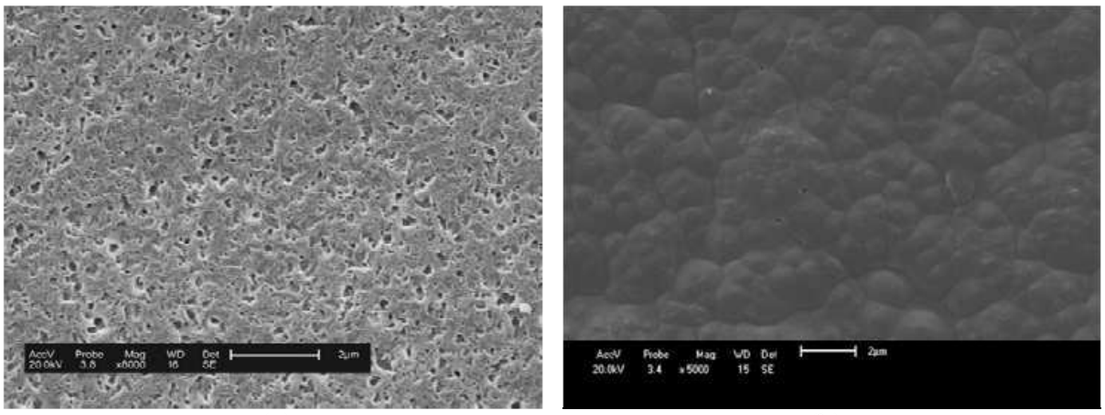

(a) (b)

Fig. 9. SEM images of the top surface of (a) PA 6/OMMT (b) PA 66/OMMT

3.4.2 Cross section

In the cross section of membranes obtained is possible to observe a variation in pore size along its thickness. For all membranes, we visualized a layer of skin and filter just below the skin to the porous layer with pores distributed uniformly spherical (Figures 10 to 12). These figures show that the skin pores filter has very small or even nonexistent, and that the porous layer has interconnected pores and well distributed. This difference in morphology in cross section that arises or is defined (also) the selectivity of the membrane, which will be investigated by measuring the flow. For all cross sections analyzed was possible to observe the formation of macrovoids and the presence of a dense skin, this probably occurred because of a delay precipitation in obtaining membrane. Generally, membranes PA 66 have a porous layer with pores much smaller when compared membranes obtained by the PA 6. The membranes of polyamide 66 and their nanocomposites present a thicker filter skin and

lower pores in the porous layer when compared to membranes made of polyamide 6. This increased thickness directly implies on the permeate flux.

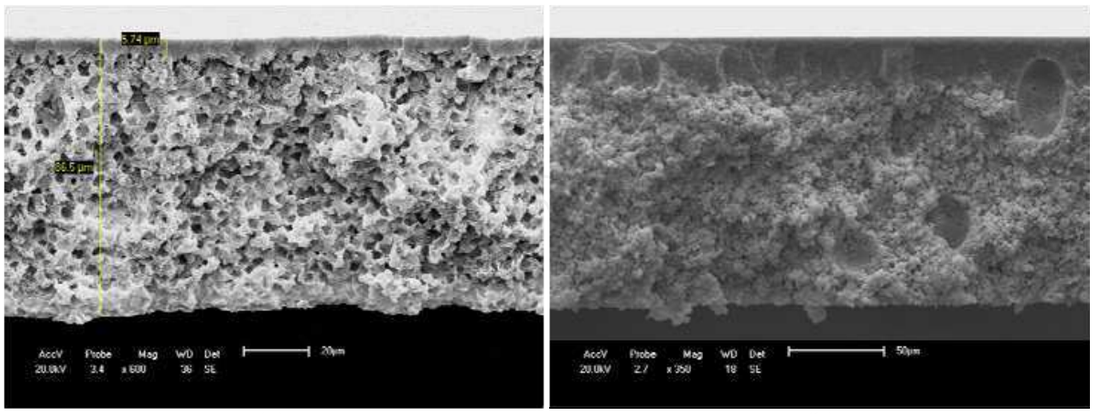

(a) (b)

Fig. 10. SEM images of the cross section of (a) PA 6 (b) PA 66

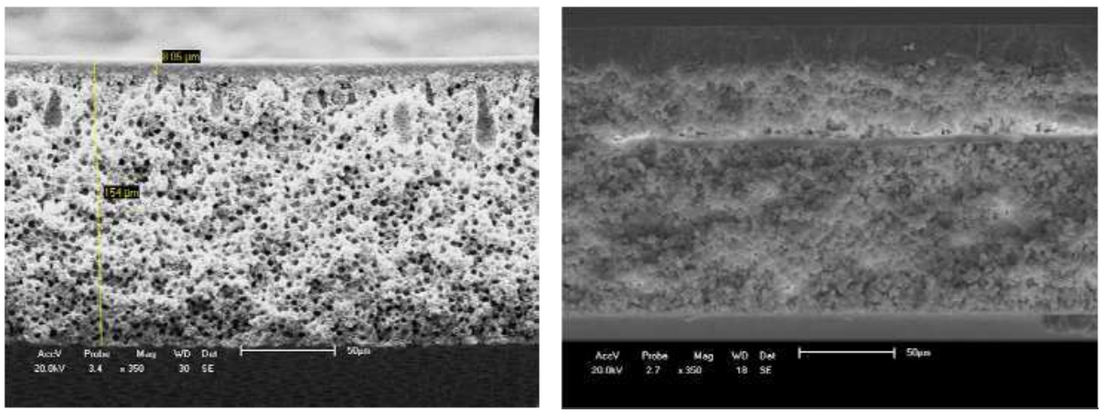

(a) (b)

Fig. 11. SEM images of the cross section of (a) PA 6/MMT (b) PA 66/MMT

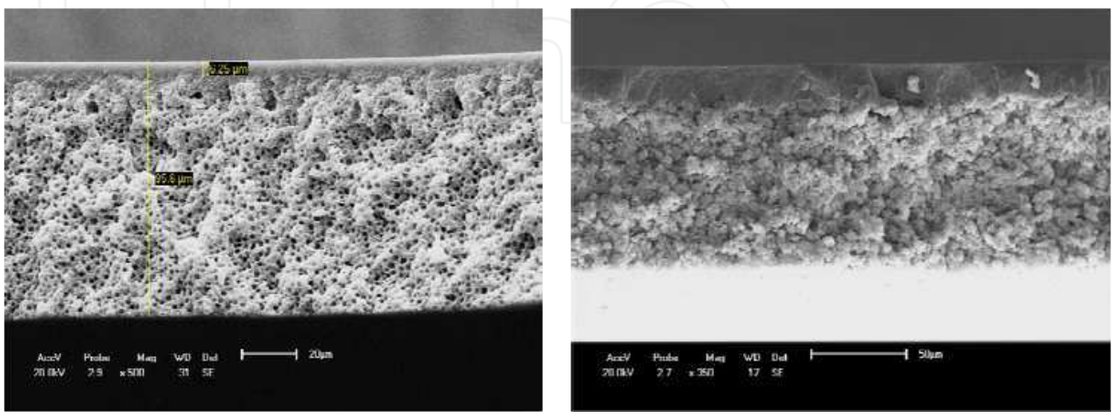

(a) (b)

Fig. 12. SEM images of the cross section of (a) PA 6/OMMT (b) PA 66/OMMT

3.5 Water flux

Figures 13 and 14 (b) show the curves of flux measurements made with distilled water in a cell filtration membranes for PA 6 and PA 66 at pressures of 0.5 and 1.0 bar respectively. For membranes of PA 6 and PA 66, the curves behave similarly, with a tendency to stay constant at low values of flow after 30 minutes. This trend can be attributed to the fact that a swelling of the matrix when in contact with water and gradually decreasing the pores, thereby precluding the permeability of water. Swelling occurred may have been caused by the hygroscopicity of the polymer used. Polyamide 6 and polyamide 66 in the form of granules showed a percentage of 1.7% absorption of water in an immersion in period of 24 hours (Wiebeck 2005).

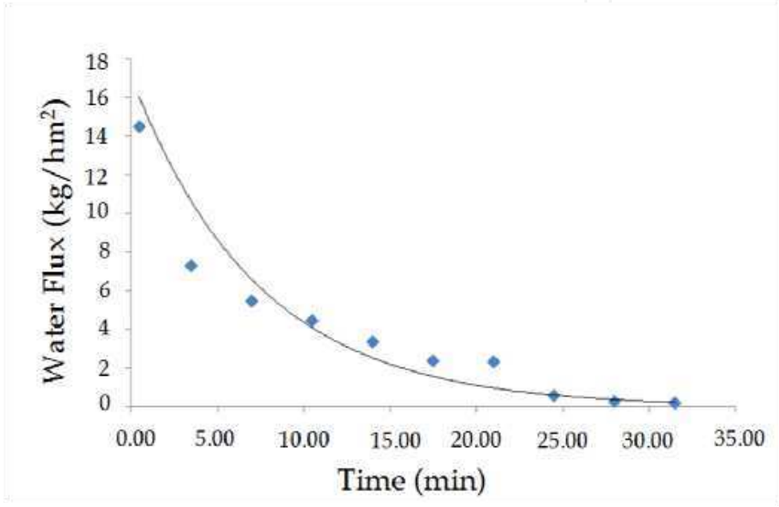

(a)

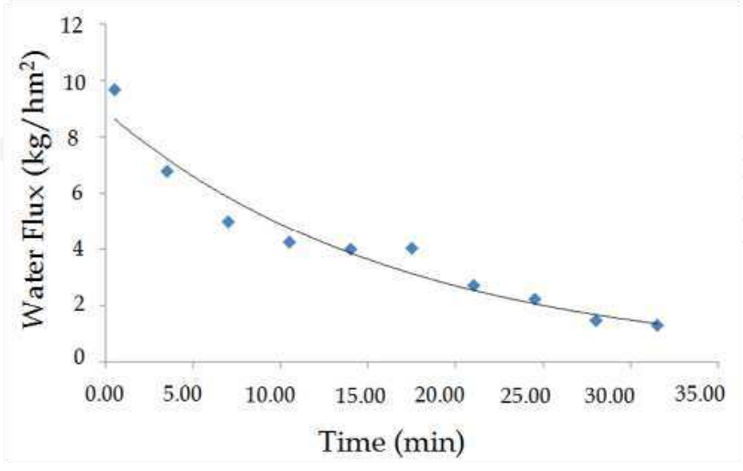

(b)

Fig. 13. Curves of water flow to the membrane of PA 6 obtained for pressures of (a) 0.5 bar and (b) 1.0 bar.

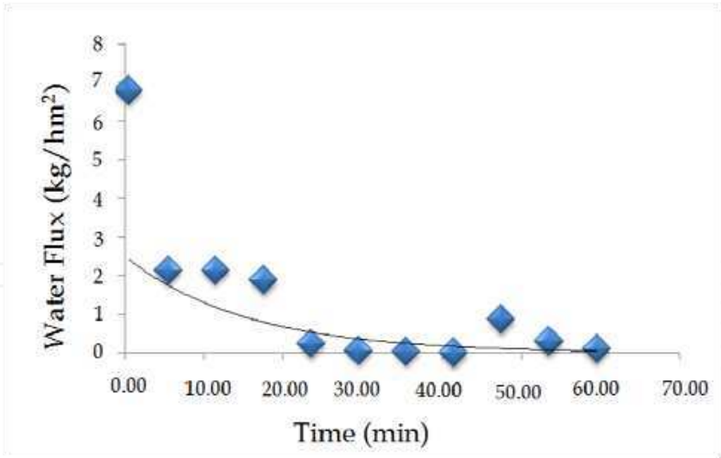

(a)

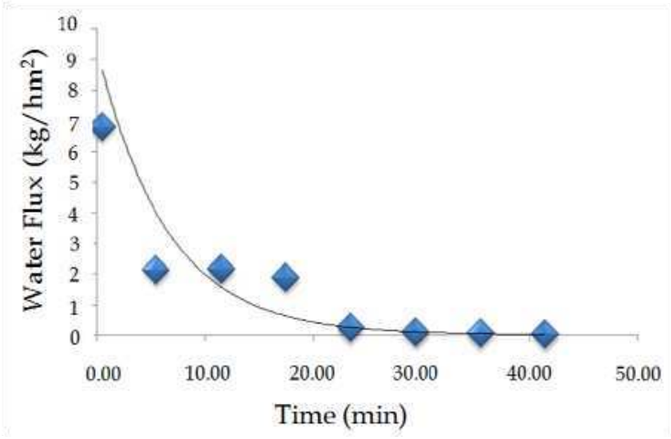

(b)

Fig. 14. Curves of water flow to the membrane of PA 66 obtained for pressures of (a) 0.5 bar and (b) 1.0 bar.

However, the membrane of PA 6 and PA 66 having a porous structure, a period of just five minutes immersed in water, swells and almost blocking the passage of water through the pores. A membrane with pores smaller and capable of swelling further reduces their pores and, consequently, the permeate flux is practically annulled. Even with the application of higher pressure, the performance remained the same, although the initial flow obtained with the membranes at a higher pressure was lower, perhaps caused by a compression of the membrane, is characteristic of the technique used in the preparation of membranes (reversed phase).

The membranes obtained from the nanocomposites, ie, where there was the presence of clay and generally larger pores compared to the membranes of PA 6 and PA 66, they were impossible to perform, even under the effect of swelling. It was hoped that the presence of clay which change the morphology of the membrane pores, favoring a better distribution and larger sizes of these, alter membrane permeability.

3. Conclusion

Based on the results obtained and presented in this study, we conclude that the presence of molecules of salt in the clay was checked by increasing interplanar basal evidenced in the XRD diffractograms, and that nanocomposites showed exfoliated and/or partially exfoliated structures, also evidenced by XRD and confirmed by the TEM photomicrographs, which showed some lamellae of clay agglomerates dispersed in polymer matrix. XRD diffractograms of the membranes confirmed the obtaning exfoliated and/or partially exfoliated structure.

SEM photomicrographs of the membranes obtained from nanocomposites present a higher amount of pores and a more uniform distribution when compared to pure polyamide membrane. Membranes of polyamide 66 present thicker skin filter. The membranes showed a low flow of distilled water and this was practically stopped in time, thus showing a swelling in the membrane structure and with increasing pressure, the initial flow was even lower, indicating it may have caused a compression of the membrane during the test. In general, asymmetric microporous membranes of PA 6, PA 66 and their nanocomposites were successfully obtained, where the presence of clay provided a considerable structural change.

4. Acknowledgment

The authors thank Rhodia/SP, Bentonit Uniao Nordeste (BUN), Clariant/PE, DEMa/UFCG, CAPES/Pro-Engenharia, CAPES/PROCAD/NF, MCT/CNPq, ANP/PRH-25 and RENAMI, for financial support.

5. References

Araujo, E. M.; Barbosa, R.; Oliveira, A. D.; Morais, C. R. S.; Melo, T. J. A.; Souza, G. A. (2007). Thermal and Mechanical Properties of PE/Organoclay nanocomposites. *J.Therm Anal Calorim.* Vol.87, pp.811-814.

Boom, R. M.; Wienk, I. M.; Boomgaard, T. V. D.; Smolders, C. A. (1992). Microstructures in phase inversion membranes. Part 2. The role of a polymeric additive. *J. Membr. Sci*. Vol. 2–3, pp. 277-292.

Bulte, A. M. W.; Mulder, M.H.V.; Smolders, C. A.; Strathmann, H. (1996). Diffusion induced phase separation with crystallizable nylons, I. Mass transfer processes for nylon 4,6. *J. Membr. Sci.* Vol.1, pp. 37-49.

Coutinho, C. M.; Chiu, M. C.; Basso, R. C.; Ribeiro, A. P. B.; Gonçalves, L. A. G.; Viotto, L. A. (2009). State of art of the application of membrane technology to vegetable oils: A review. *Food. Res.* Vol.42, pp.536-550.

Dubois, A. L. (2000). Polymer-layered silicate nanocomposites :preparation, properties and uses of a new class of materials. *Mat. Sci. Eng.* Vol.28, pp.1-63.

Fornes, T. D.; Yoon, P. J.; Keskkula, H.; Paul, D. R. (2001). Nylon 6 nanocomposites: the effect of matrix molecular weight. *Polymer.* Vol.42, No.25, pp.9929-9940.

Habert, A. C.; Borges, C. P.; Nobrega, R. (2006). Processos de separação por membranas. Rio de Janeiro: E-papers.

Herrero, M. ; Benito, P. ; Labajos, F. M. ; Rives, V. ; Zhu, Y. D. ; Allen, G. C. ; Adams, J. M. (2010). Structural characterization and thermal properties of polyamide 6.6/Mg,Al/adipate-LDH nanocomposites obtained by solid state polymerization. *J. Sol. Stat. Chem.* Vol. 183, pp1645-1651.

Khanna, Y.P.; Khun, W.P. (1997). Measurement of crystalline index in nylons by DSC: Complexities and recommendations. *J. Polym. Sci.* Vol. 35, pp.2219-2231.

Kohan, I. M. (1995). *Nylon Plastics Handbook.* Hanser Publishers, Munich Vienna, New York.

Lagaly, G. (1999). Introduction: from clay mineral–polymer interactions to clay mineral–polymer nanocompósitos. *Polymer.* Vol.15. No.1-2, pp,1-9.

LeBaron, P. C. ; Wang, Z. ; Pinnavaia, T. J. (1999). Polymer-layered silicate nanocomposites: an overview. *Polymer*, Vol.15. No.1-2, pp,11-29.

Lee, W. D.; Im, S. S.; Lim, H. M.; Kim, K. J. (2006). Preparation and properties of layered double hydroxide/poly(ethylene terephthalate) nanocomposites by direct melt compounding. *Polymer.* Vol 47, No. 4, pp. 1364-1371.

Leite, A. M. D.; Maia, L. F.; Paz, R. A.; Araujo, E. M.; Lira, H. L. (2009). Thermal properties from membrane of polyamide 6/ montmorillonite clay nanocomposites obtained by immersion precipitation method. *J.Therm Anal Calorim.* Vol.97, pp.577-580.

Lin, L.; Rhee, K. C.; Koseoglu, S. S. (1997). Bench-scale membrane degumming of crude vegetable oil: Process optimization. *J. Membr. Sci.* Vol. 134, pp.101–108.

Liu, Y ; Yang, G. (2009). Non-isothermal crystallization kinetics of polyamide-6/graphite oxide nancomposites. *Thermochim. Acta,* Vol.500, pp. 13-20.

Lu, X. F.; Hay,J. N. (2001). Isothermal crystallization kinetics and melting behaviour of poly (ethylene terephthalate). *Polymer*, Vol. 42 No. 23, pp.9423–9431.

Nagarale, R. K.; Shashi, V. K.; Rangarajan, R. (2005). Preparation of polyvinyl alcohol-silica hybrid heterogeneous anion-exchange membranes by sol-gel method and their characterization. *J. Membr. Sci.* Vol.248, pp. 37-44.

Pfaendner, R. (2010). Nanocomposites : Industrial opportunity or challenge ?. *Polym. Degrad. Stab*. Vol.95, pp.369-373.

Qiu, L.; Chen, W.; Qu, B. (2006). Morphology and thermal stabilization mechanism of LLDPE/MMT and LLDPE/LDH nanocompósitos. *Polymer.* Vol.47, No. 14, pp. 922-930.

Run,M.T. ; Wu, S. Z. ; Zhang, D.Y. ; Wu, G. (2005). Melting behaviors and isothermal crystallization kinetics of poly(ethylene terephthalate)/mesoporous molecular sieve composite. *Polymer*, Vol. 46. No. 14, pp.5308–5316.

Ulbricht, M. (2006). Advanced functional polymer membranes. *Polymer.* Vol. 47, No.7, pp.2217-2262.

Uragami, T.; Matsugi, H.; Miyata, T. (2005). Pervaporation characteristics of organic-inorganic hybrid membranes composed of poly(vinyl alcohol-co-acrylic acid) and tetraethoxysilane for water/ethanol separation. *Macromolecules*. Vol. 38, pp.8440-8446.

Varlot, K.; Reynaud, E.; Kloppfer, M. H. ; Vigier, G. ; Varlet, J. (2001). Clay-Reinforced Polyamide : Preferential Orientation of the Montmorillonite Sheets and the Polyamide Crystalline Lamellae. *Pol. Sci.B*. Vol.39, pp.1360-1370.

Wang, G. A.; Wang, C. C.; Chen, C. Y. (2005). The disorderly exfoliated LDHs/PMMA nanocomposite synthesized by in situ bulk polymerization. *Polymer*. Vol. 46, No.14, pp.5065-5074.

Wiebeck, H.; Harada, J. (2005). *Plásticos de engenharia: Tecnologia e aplicações.* 1a ed., Artliber Editora Ltda, Brazil.

Witte, P. V.; Dijkstra, P. J.; Van Den Berg, J. W. A.; Feijen, J. (1996). Phase separation processes in polymer solutions in relation to membrane formation. *J. Membr. Sci*. Vol. 1-2, pp. 1-31.

Xi, Y.; Frost, R.L.; He, H.; Kloprogge, T.; Bostrom, T. (2005). Modification of Wyoming montmorillonite surfaces using a cationic surfactant. *Langmuir*, Vol. 21, pp.-8675–8680.

Yang, Y.; Zhang, H.; Wag, P.; Zheng, Q.; Li, J. (2007). The influence of nano-sized TiO2 fillers on the morphologies and properties of PSF UF membranes. *J. Membr. Sci.* Vol.288, pp. 231-238.

Zhao, F.; Bao, X.; McLauchilin, A. R.; Gu, J.; Wan, C.; Kandasubramanian, B. (2010). Effect of POSS on morphology and mechanical properties of polyamide 12/montmorillonite nanocompósitos. *Appl.Clay.* Vol 47, pp.249-256.

IntechOpen

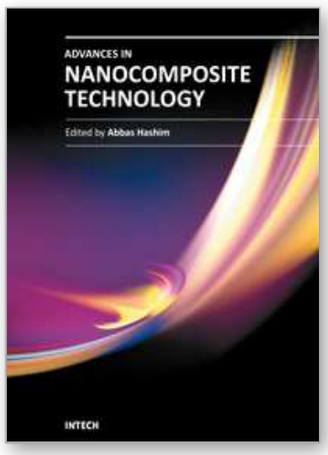

Advances in Nanocomposite Technology

Edited by Dr. Abbass Hashim

ISBN 978-953-307-347-7
Hard cover, 374 pages
Publisher InTech
Published online 27, July, 2011
Published in print edition July, 2011

The book â€œAdvances in Nanocomposite Technologyâ€ contains 16 chapters divided in three sections. Section one, â€œElectronic Applicationsâ€, deals with the preparation and characterization of nanocomposite materials for electronic applications and studies. In section two, â€œMaterial Nanocompositesâ€, the advanced research of polymer nanocomposite material and polymer-clay, ceramic, silicate glass-based nanocomposite and the functionality of graphene nanocomposites is presented. The â€œHuman and Bioapplicationsâ€ section is describing how nanostructures are synthesized and draw attention on wide variety of nanostructures available for biological research and treatment applications. We believe that this book offers broad examples of existing developments in nanocomposite technology research and an excellent introduction to nanoelectronics, nanomaterial applications and bionanocomposites.

How to reference

In order to correctly reference this scholarly work, feel free to copy and paste the following:

Edcleide Araujo, Amanda M. D. Leite, Vanessa Da N. Medeiros, Rene Anisio Paz and Helio De L. Lira (2011). Comparative Study of Membranes Obtained from PA6 and PA66/National Clay Nanocomposites, Advances in Nanocomposite Technology, Dr. Abbass Hashim (Ed.), ISBN: 978-953-307-347-7, InTech, Available from: http://www.intechopen.com/books/advances-in-nanocomposite-technology/comparative-study-of-membranes-obtained-from-pa6-and-pa66-national-clay-nanocomposites

INTECH
open science | open minds

InTech Europe
University Campus STeP Ri
Slavka Krautzeka 83/A
51000 Rijeka, Croatia
Phone: +385 (51) 770 447
Fax: +385 (51) 686 166
www.intechopen.com

InTech China
Unit 405, Office Block, Hotel Equatorial Shanghai
No.65, Yan An Road (West), Shanghai, 200040, China
中国上海市延安西路65号上海国际贵都大饭店办公楼405单元
Phone: +86-21-62489820
Fax: +86-21-62489821

© 2011 The Author(s). Licensee IntechOpen. This chapter is distributed under the terms of the Creative Commons Attribution-NonCommercial-ShareAlike-3.0 License, which permits use, distribution and reproduction for non-commercial purposes, provided the original is properly cited and derivative works building on this content are distributed under the same license.

IntechOpen

IntechOpen